

**X-ray Light Curve of the
Sgr A* Active History
by 3D View of X-ray Reflection Nebulae**

劉 周強 (京都大学 D3)

ryu@cr.scphys.kyoto-u.ac.jp

I. Introduction : Unrevealed History of SMBH in the GC

In the the Galactic center (GC) region at 8 kpc, we have discovered strong emission lines (the 6.4 keV line; Fig.1 top) from neutral irons in molecular clouds (MCs) of Sgr B and Sgr A, and flux variabilities in a time scale of a few years. We then propose the X-ray reflection Nebulae(XRNe) scenario that the MCs produce the 6.4 keV line by reflection and/or fluorescent of irradiating X-rays from a past flare of the super massive black hole (Sgr A*) about several hundreds years ago (Koyama+96, Inui+08, Ponti+10, Nobukawa+11).

To extend this scenario, using Suzaku, Ryu et al. 2009 developed a methodology to study the line-of-sight position of the XRNe in the Sgr B region using the X-ray absorption feature of the GC hot plasma (Koyama +89, Uchiyama+1; Fig.1 bottom). In this work, we complete the the methodology and applied it to another XRNe of Sgr C (Nakajima+08), and investigate the past activities of Sgr A* using the three dimensional (3D) position of multi-XRNe in Sgr C and Sgr B.

I. Introduction : Unrevealed History of SMBH in the GC

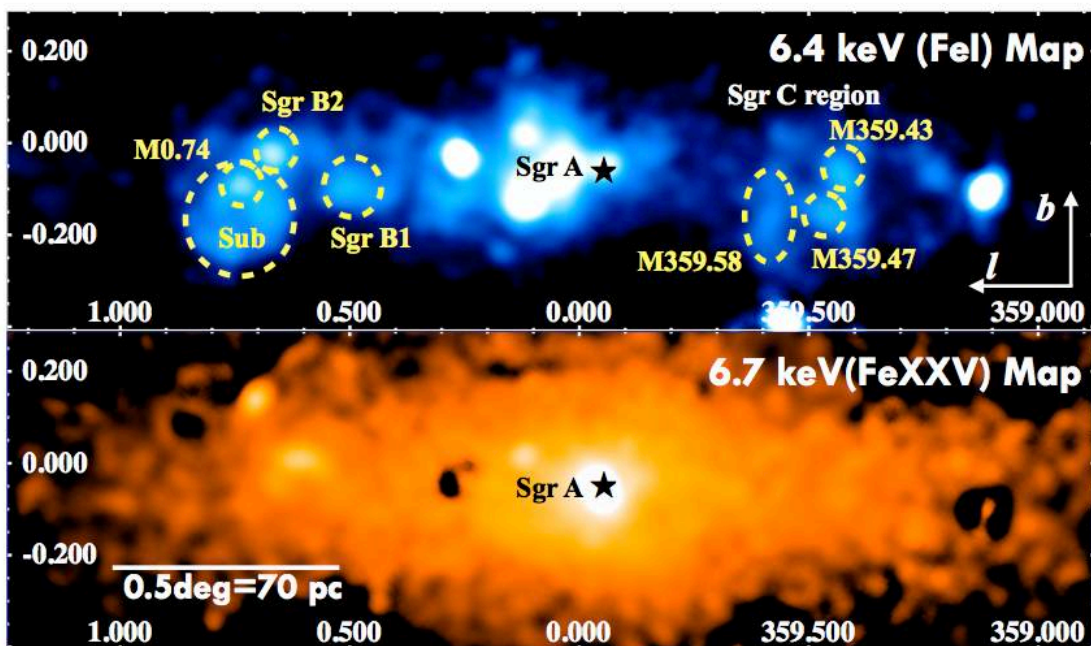


Fig.1. XRNe (top) and hot plasma (bottom) in GC.

II. Analyses : How to Measure the Line-of-sight (LOF) Position of XRNe

Step 1 : Modeling of X-ray Emission toward GC

In Fig.2, we show the face-on view of X-ray components along the line of sight. The X-ray spectrum model can be formed as below (Ryu+09, Nobu+10),

$$\text{Flux (E)} = \text{Abs1} \times (\text{GC-Plasma-E} \times \text{R}) + \text{Abs1} \times \text{Abs2} \times (\text{GC-Plasma-E} \times (1-\text{R}) + \text{XRNE}) + \text{Foreground-E} + \text{CXB}$$

- GCPE= APEC(0.87keV)+APEC(6.5keV); ratio=0.27
 - XRNE= PowLaw+Gaus(6.4 keV)+Gaus(7.05 keV); EW=1.6 keV, Photon Index=1.7
- => Free parameters are Abs1 (NH: ISM), Abs2(NH: XRN), 6.4 keV Flux, and R.

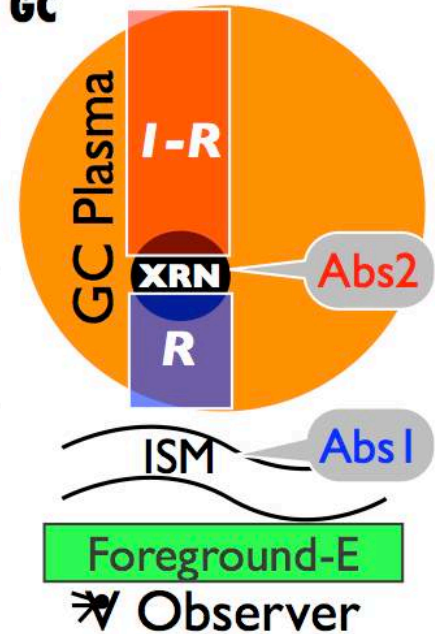


Fig.2. X-ray components in LOF toward GC .

II. Analyses : How to Measure the Line-of-sight (LOF) Position of XRNe

Step 2 : Fitting of XRNe Spectra

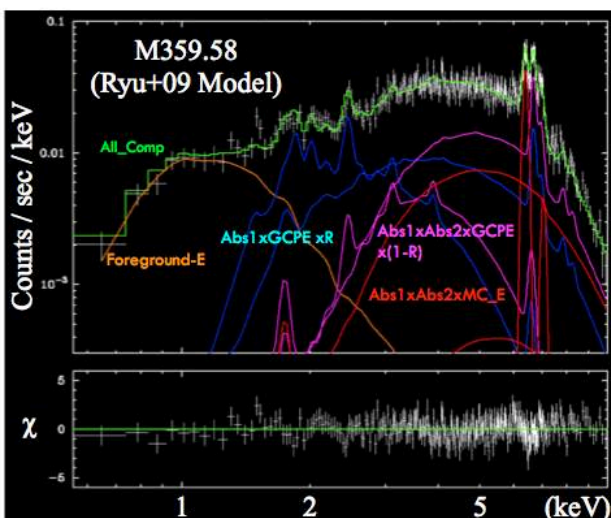


Fig3. Spectral fitting results of XRNe (M 358.58) in Sgr C.

From the Suzaku archive data, we extracted spectra for three XRNe in Sgr C (Fig1. top) from the Suzaku XIS data. As an fitting example shown in Fig.3, the spectrum of XRNe (M359.58) is well explained by the model set in Step1.

In Table 1, we show the best-fit parameter for R which indicates the LOF position (c.f., Fig.2).

Table 1	M359.58	M359.47	M359.43
R (90% Errors)	0.27 (0.2-0.3)	0.58 (0.4-0.7)	0.17 (0.1-0.3)

II. Analyses : How to Measure the Line-of-sight (LOF) Position of XRNe

Step 3 : Modeling of GC Plasma Emission Spatial Distribution

In Fig.4, we constructed model for the symmetrical spatial distribution of the GC plasma emission, GCPE(X,Y,Z), from the results of Uchiyama+II using the Fe-XXV (6.7 keV) line.

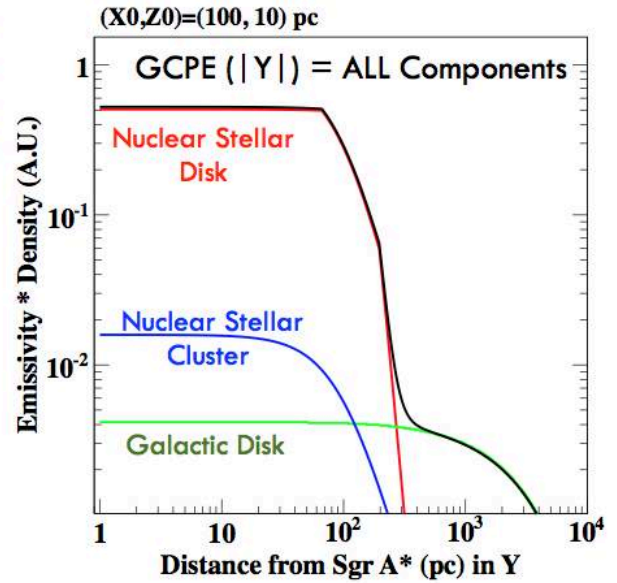
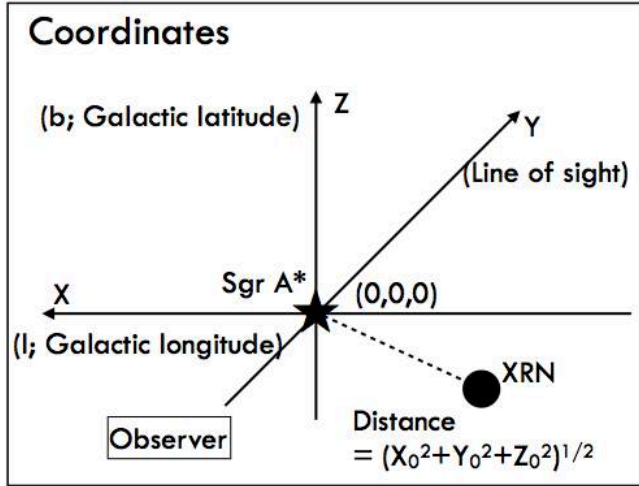


Fig.4. GCPE profile in Y(LOF) .

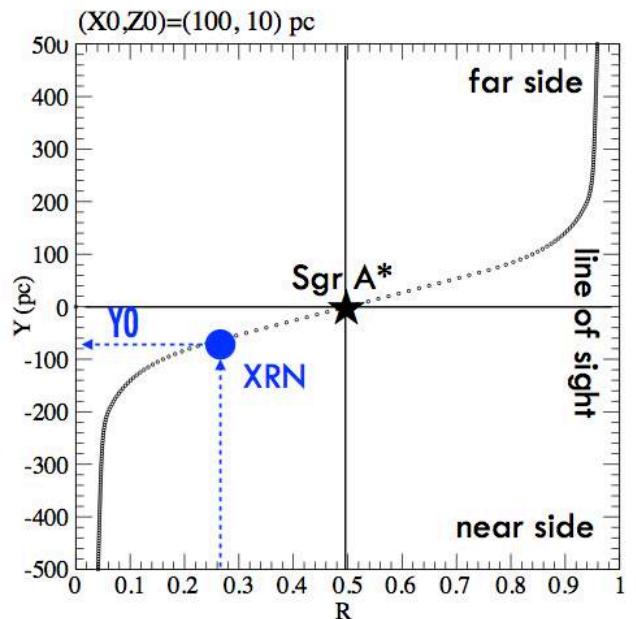
II. Analyses : How to Measure the Line-of-sight (LOF) Position of XRNe

Step 4 : Calculation of the Line-of-sight Position from R

The relation between the the R parameter and the LOF position of an XRNe (=Y₀) is expressed as below,

$$R(Y_0) = \frac{\int_{-\infty}^{Y_0} \text{GCPE}(X_0, Z_0, Y) dY}{\int_{-\infty}^{\infty} \text{GCPE}(X_0, Z_0, Y) dY}$$

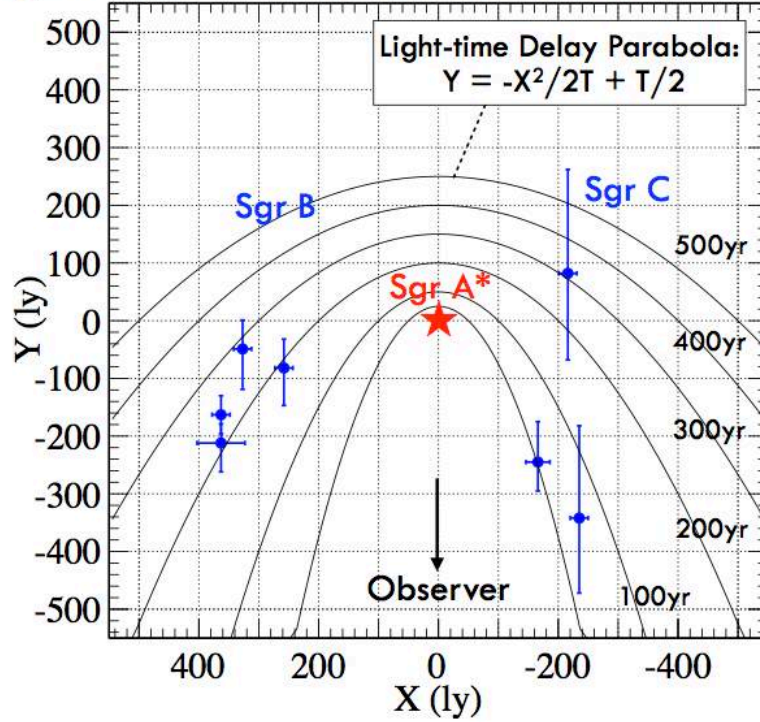
Y₀ can be determined by the l-b position of XRNe at (X₀, Z₀) in GCPE (Step3) and the best-fit parameter R obtained in Step2. We show an example of R(Y₀) in Fig.5.



III. Results : Face-on View of XRNe and Past Activity of Sgr A*

Using the methods described in Sec-II, we measured LOF position of XRNe in Sgr B and Sgr C. The face-on view is shown in Fig. 5.

Fig.5. Face-on View of XRNe around Sgr A*



III. Results : Face-on View of XRNe and Past Activity of Sgr A*

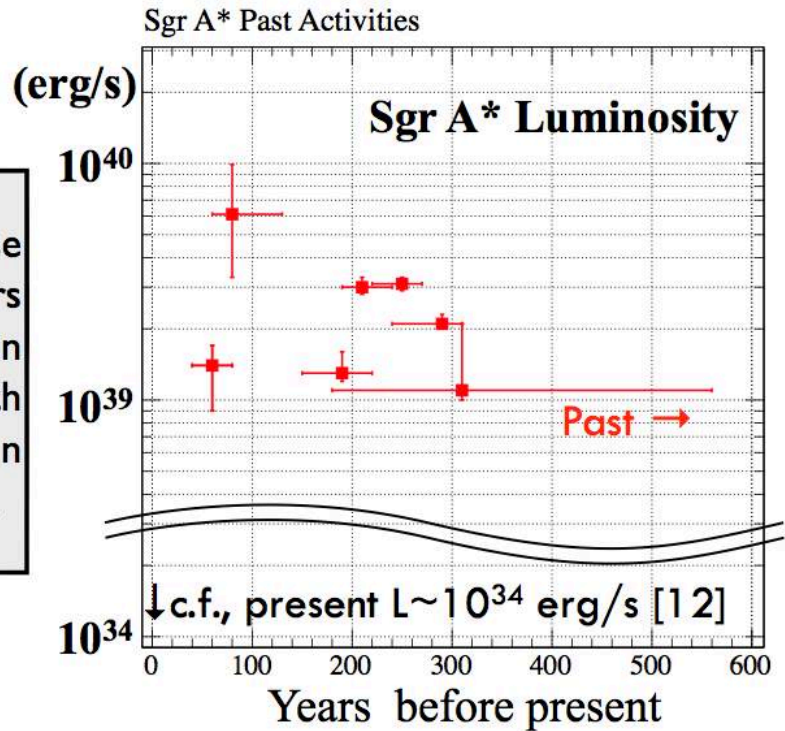
The required luminosity of Sgr A* can be calculated from parameters of XRNe in the following formula (e.g. Nobukawa et al. 2008, Sunyaev+98):

$$L_{\text{req}} = 2 \times (I_{6.4 \text{ keV}} / 2.8 \text{ e}^{-5} \text{ cm}^{-2} \text{ s}^{-1}) \times (\text{Distance} / 100 \text{ pc})^2 \times (N_{\text{H}} / 9 \text{ e}^{22} \text{ cm}^{-2})^{-1} \times (\text{Area} / 119 \text{ pc}^2)^{-1} \quad [10^{39} \text{ erg s}^{-1}]$$

Table 2	M0.66 (Sgr B2)	M0.51 (Sgr B1)	M0.74 (Sgr B)	M0.74-sub (Sgr B)	M359.43 (Sgr C)	M359.47 (Sgr C)	M359.58 (Sgr C)
Distance (pc)	101	84	122	130	127	72	92
N_{H} (e22 cm ⁻²)	36.5	12	23	11.5	6.5	11	9.8
6.4 keV Intensity (ph /s/cm ²)	6.4E-05	2.3E-05	4.2E-05	1.3E-04	2.1E-05	2.0E-05	5.8E-05
Surface area (pc ²)	67	77	67	474	67	67	280
L_{SgrA^*} (erg/s)	2.1E+39	1.3E+39	3.1E+39	3.0E+39	6.1E+39	1.1E+39	1.4E+39
Time delay (yr)	290	190	250	210	80	310	60

III. Results : Face-on View of XRNe and Past Activity of Sgr A*

Sgr A* was in an active phase during the past 60-500 years (Fig.6); the luminosity was in range of 10^{39} - 10^{40} erg/s, with decade-scale variability in factor of 2-3 (i.e., multi-flare).



References

- [1] Koyama K., et al. 1996, PASJ, 48, 249
- [2] Inui T. et al. 2009, PASJ, 61, 241
- [3] G. Ponti et al. 2010, APJ. 714
- [4] Nobukawa et al. 2011, APJ, submitted
- [5] S.G.Ryu et al. 2009, PASJ, 61, 751
- [6] K.Koyama et al. 1989, Nature, 339, 603
- [7] Uchiyama et al. 2011, PASJ, submitted
- [8] Nakajima et al. 2008, PASJ
- [9] Nobukawa et al. 2010, PASJ, 62, 423
- [10] Sunyaev, R., & Churazov, E. 1998, MNRAS, 297, 1279
- [11] Baganoff et al., 2003, APJ, 591, 891